Neural Networks, Vol. 4, pp. 3-13, 1991
Printed in the USA.

0893-6080/91 $3.00 + .00

ORIGINAL CONTRIBUTION

A Visual Cortex Domain Model and Its Use for Visual Information Processing

ILYA A. RYBAK, NATALIA A. SHEVTSOVA, LUBOV N. PODLADCHIKOVA, AND ALEXANDER V. GOLOVAN

Institute of Neurocybernetics at Rostov State University, USSR

(*Received 8 May 1989; revised and accepted 9 August 1990*)

Abstract—*A model of an iso-orientation domain in the visual cortex is developed. The iso-orientation domain is represented as a neural network with retinotopically organized afferent inputs and anisotropic lateral inhibition formed by feedbacks via inhibitory interneurons. Temporal dynamics of neuron responses to oriented stimuli is studied. The results of computer simulations are compared with those of neurophysiological experiments. It is shown that the later phase of neuron response has a more sharp orientation tuning than the initial one. It is suggested that the initial phase of neuron response encodes intensity parameters of visual stimulus, whereas the later phase encodes its orientation. The design of the neural network preprocessor and the architecture of the system for visual information processing, based on the idea of parallel-sequential processing, are proposed. The example of a test image processing is presented.*

Keywords—Visual cortex, Neural network, Lateral inhibition, Iso-orientation domain, Feature extraction, Orientation filtration, Multiresolution image processing.

1. INTRODUCTION

Image recognition research is focused mainly on two problems: 1) elaboration of effective algorithms of image analysis and description, and 2) investigation of the visual system mechanisms. It is still unclear whether these two problems should be distinguished. Some researchers assume that structure and mechanisms used by natural visual system cannot be applied to computer vision. On the contrary, others think that it is necessary to elucidate subtle mechanisms of visual perception to develop new computer vision system architectures. Nevertheless, most researchers come to the conclusion that the von-Neuman architecture does not allow to create computer vision systems comparable with human visual systems in effectiveness (Levialdi, 1983).

It is well known that when images are analyzed with the help of conventional computers of sequential type, most of the time is spent on preliminary processing of bulky input information. Parallel preprocessing and initial data compressing are the main means of reduction of the time of visual information processing. In recent years, a trend manifested itself to create parallel-type systems for visual information analysis with multiprocessor architecture. However, parallel processing cannot solve all the problems of computer vision. Minsky (1975) contends that parallelism is effective at lower levels of information processing dealing with feature extraction, whereas its useful effects have serious limitations at higher levels. Not even high computational efficiency achievable by parallel computing circuits can solve such problems as invariance of feature detection and estimation of contexts at different levels of abstraction (Kohonen, 1988).

It is now a widely-held view that visual perception is based on two interrelated processes: parallel processing of visual information carried out automatically by mechanisms determined by neuronal organization of the retina, lateral geniculate nucleus, and visual cortex; and sequential processing related to image recognition mechanisms and controlled by attention (Julesz, 1975; Neisser, 1967; Shiffrin & Schneider, 1977). In the first process, detector properties of single neurons and local neuron nets are of primary importance. In the second process, eye movements are considered to be an essential factor.

Acknowledgements: The authors thank Vladislav M. Sandler and Tatjana M. Bogatyreva for their participation in discussions, valuable assistance in the preparation of the manuscript and illustrations.

Requests for reprints should be sent to Ilya A. Rybak, Institute of Neurocybernetics, Rostov State University, 194/1 Stachka Ave., Rostov-on-Don 344104, USSR.

As a result of these movements, the most informative parts of the image are sequentially projected onto the fovea for fine processing (Burt, 1988; Yarbus, 1965). During the second process, a tuning of detector properties of low-level neurons can be controlled by high-level structures. Thus, the purposeful feature extraction for image recognition is provided.

Therefore, the adequate computer system for the processing and analysis of visual information should include a preprocessor with a neural network architecture, simulating parallel information processing at low levels of the visual system, and a sequential type computer tuning the preprocessor to obtain necessary information for image recognition.

The development of the neural network preprocessor should be preceded by a study on neuronal organization of low-level structures of the visual system and their mathematical modelling and computer simulation. As noted above, these structures primarily accomplish a preliminary processing of information, including filtration and encoding of image features. However, it is not obvious what features are encoded by neurons of these structures and what mechanisms underlie the encoding. Orientation of edges and contour elements of an image is considered to be one of the main features detected by neurons of the primary visual cortex (Hubel & Wiesel, 1962, 1974). Orientation-selective properties of these neurons make it possible to encode orientations of image elements and to compress initial information (Kunt, Ikonomopoulos, & Kocher, 1985).

2. ISO-ORIENTATION DOMAIN IN THE VISUAL CORTEX

It is well known that neighbor neurons in the visual cortex have a similar orientation tuning and form an orientation-selective column, or an iso-orientation domain. A set of orientation columns with a common receptive field forms a topical module of the cortex—a hypercolumn (Hubel & Wiesel, 1962, 1974). Besides, visual cortex afferents are organized retinitopically (Talbot & Marshall, 1941) and it is believed that in addition to global mapping, there are retinotopically-organized projections of the common receptive field of a hypercolumn onto each iso-orientation domain (Schwartz, 1980).

To date, there are several assumptions about the mechanisms of orientation selectivity in the visual cortex (Baxter & Dow, 1989; Braitenberg & Braitenberg, 1979; Finette, Harth, & Csermely, 1978; Hubel & Wiesel, 1962, 1974; Linsker, 1986a, 1986b; Malsburg, 1973; Malsburg & Cowan, 1982; Paradiso, 1988; Sillito, 1984; Vidyasagar, 1987). Evidently, the mechanism of orientation selectivity of cortical neurons is related to anisotropic distribution of some fibers. The first explanation of this mechanism was based on the idea of anisotropic distribution of afferent fibers forming specifically-elongated receptive fields of cortical neurons (Hubel & Wiesel, 1962). Another idea supposed anisotropic lateral excitation in an iso-orientation domain (Finette, Harth, & Csermely, 1978). However, experiments of Sillito (1975, 1984) showed that orientation selectivity of cortical neurons decreased or disappeared when intracortical inhibition had been blocked by bicuculline. This fact supports the idea that the anisotropy of lateral inhibitory connections may be the primary mechanism of orientation selectivity (Benevento, Creutzfeldt, & Kuhnt, 1972; Creutzfeldt, Kuhnt, & Benevento, 1974).

An abundance of neuroscience data indicate that afferent fibers form only excitatory synaptic contacts in the cortex and inhibition is mediated via intracortical connections of inhibitory interneurons (Benevento, Creutzfeldt, & Kuhnt, 1972; Ferster & Lindstrom, 1983; Garey & Powell, 1971; Hess, Negishi, & Creutzfeldt, 1975; Ito, 1970; Stefanis & Jasper, 1964; Watanabe, Konishi, & Creutzfeldt, 1966). Lateral inhibition may be of direct type when afferent fibers have excitatory synaptic contacts with inhibitory neurons or backward type when inhibitory interneurons are activated by axon collaterals from cells excited by afferent inputs (Eccles, 1969; Supin, 1970). In some studies, evidence of backward character of lateral inhibition in the visual cortex was revealed (Hayashi, 1969; Supin, 1970; Watanabe, Kohishi, & Creutzfeldt, 1966).

Thus, an iso-orientation domain of the visual cortex may be regarded as a neural structure with retinotopically-organized afferent inputs and anisotropic lateral inhibition formed by feedbacks via inhibitory interneurons.

3. THE MODEL OF AN ISO-ORIENTATION DOMAIN OF THE VISUAL CORTEX

A great number of models of neural structures with lateral inhibition were elaborated (Amari, 1977, 1982; Wilson & Cowan, 1972, 1973 and many others). However, anisotropy of connections and dynamics of responses to oriented stimuli were not considered in these studies. On the other hand, in most studies devoted to modelling of orientation selectivity of cortical neurons, the mechanism of selectivity is suggested to be a result of either spatial organization of input afferent fibers or anisotropy of lateral intracortical excitatory connections (Finette, Harth, & Csermely, 1978; Grossberg, Mingolla, & Todorovic, 1989; Linsker, 1986a, 1986b; Malsburg, 1973; Malsburg & Cowan, 1987). The development of neural structure with anisotropy of lateral inhibition and examination of its responses to oriented stimuli was the goal of the current study.

As an element of such a structure, we used a model of a neuron described by

$$T_i \frac{d}{dt} U_i(t) = -U_i(t) + \sum_j q_{ij} Z_j(t) + q_i^s Z_i^s(t) + S_i - h_i; \quad (1)$$

$$Z_i(t) = f[U_i(t)], \quad (2)$$

where $U_i(t)$ is membrane potential of the i-th neuron; $Z_i(t)$ is its output variable (frequency of impulses); h_i is threshold ($h_i > 0$); q_{ij} is synaptic weight of the j-th input to the i-th neuron; q_i^s is synaptic weight of the external input; $Z_i^s(t)$ is test input influence; S_i is uncontrollable input influence which determines the initial level of membrane potential; T_i is time constant; t is time variable; f is nonlinear function

$$f[U] = \begin{cases} kU & \text{if } U \geq 0; \\ 0 & \text{if } U < 0, \end{cases} \quad (3)$$

where $k > 0$.

The system under consideration included a two-dimensional neural structure and a flat receptor layer of $N \times N$ elements (S-layer). For convenience, the neural structure was subdivided into two flat layers of $N \times N$ elements: a layer of excitatory elements (E-layer), and a layer of inhibitory interneurons (I-layer) (Figure 1). Each element in E-layer had an excitatory input from the corresponding element in S-layer and eight excitatory inputs from its neighbors in E-layer. The former input provided a topical mapping $S \rightarrow E$ and the latter inputs resulted in isotropy of lateral excitation within E-layer. Besides, each E-layer element was inhibited by the corresponding interneuron in I-layer (Figure 1a). Each I-layer element had an excitatory input from the corresponding E-layer element and excitatory inputs from some other E-layer elements. The former input provided self-inhibition of E-layer element, the latter inputs resulted in anisotropic backward inhibition (Figure 1b).

The structure under consideration is described as follows:

$$\begin{cases} T_E \frac{d}{dt} U_{ij}^E(t) = -U_{ij}^E(t) + q^{EE} \\ \qquad \times \sum\limits_{\substack{k=i-1 \\ (k,l)\neq(i,j)}}^{i+1} \sum\limits_{l=j-1}^{j+1} Z_{kl}^E(t) - q^{IE} Z_{ij}^I(t) \\ \qquad + q^{SE} Z_{ij}^S(t) + S_E - h_E; \\ T_I \frac{d}{dt} U_{ij}^I(t) = -U_{ij}^I(t) + q_0^{EI} Z_{ij}^E(t) + q^{EI} \\ \qquad \times \sum\limits_{\substack{k,l \in \Omega_{ij}(\varphi) \\ (k,l)\neq(i,j)}} \sum Z_{kl}^E(t) + S_I - h_I; \\ Z_{ij}^E(t) = f[U_{ij}^E(t)]; \\ Z_{ij}^I(t) = f[U_{ij}^I(t)]; \qquad i, j = 1, \ldots, N, \end{cases} \quad (4)$$

where indices "E" and "I" at neuron parameters and variables indicate that given neuron belongs to E or I-layer; indices "EE", "IE", "EI", "SE" refer to weights of synaptic connections: the first letter here stands for the layer position of the postsynaptic neuron, while the second letter stands for that of the presynaptic neuron. The shape of area $\Omega_{ij}(\varphi)$ of E-layer elements, forming the excitatory inputs to the (i,j)-th I-layer neuron, determines anisotropy of lateral inhibition corresponding to orientation φ. Examples of the areas $\Omega_{ij}(\varphi)$ are schematically depicted in Figures 2b–e. Figure 2a shows an interneuron with anisotropically ramificated dendritic tree capable to produce anisotropic lateral inhibition. The inhibition like that may be provided also by anisotropic distribution of recurrent collaterals of excitatory cells.

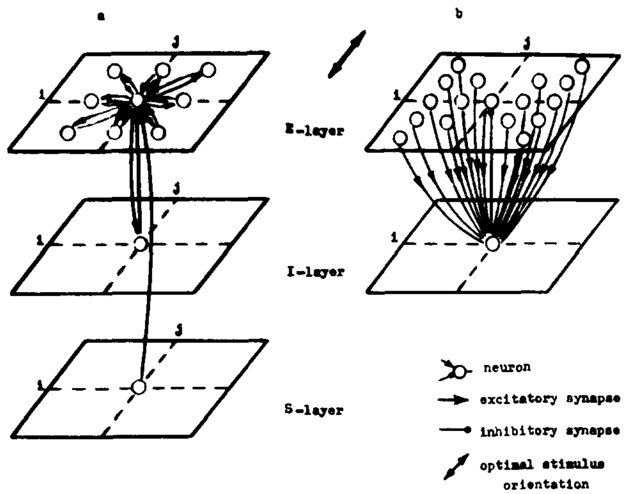

FIGURE 1. Model of the iso-orientation domain in the visual cortex: a) connections of a E-layer neuron; b) connections of a I-layer neuron.

Earlier, simple neural network being elementary parts of the considered structure were studied analytically (Rybak, 1988; Rybak, Shevtsova, Podladchikova, Golovan, & Markarov, 1987). On the basis of these studies, synaptic weights q^{EI}, q_0^{EI}, q^{EI}, q^{EE} were chosen under the conditions

$$\beta > \beta_0 + 1 + \alpha; \qquad \alpha < 1, \quad (5)$$

where

$$\beta_0 = q_0^{EI} q^{IE} k^2; \qquad \beta = q^{EI} q^{IE} k^2; \qquad \alpha = 8 q^{EE} k. \quad (6)$$

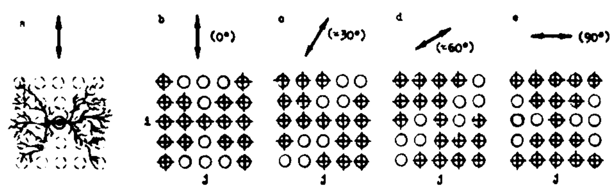

FIGURE 2. Anisotropy of lateral connections; a) inhibitory interneuron with anisotropic dendritic tree; b–e) shapes of areas $\Omega_{ij}(\varphi)$ for different optimal stimulus orientations. The cross mark indicates E-layer neurons which innervate the (i,j)-th interneuron. The stimulus optimal orientations are shown by arrows for each φ.

It is generally agreed that time constants of inhibitory neurons are greater than those of excitatory neurons

$$T_I > T_E. \quad (7)$$

Besides, all neurons were supposed to be on the brink of excitation

$$\begin{cases} S_E - h_E = 0; \\ S_I - h_I = 0. \end{cases} \quad (8)$$

The dynamics of neuron responses to oriented input stimuli was studied in computer simulations. The system of equations (4) was solved by the Runge-Kutta algorithm. Stimuli, switched on at $t = 0$, were presented as a configuration of S-layer excited elements. At $t \geq 0$, $Z_{ij}^S(t) = Z_m$ for excited elements, and $Z_{ij}^S(t) = 0$ for others. Strips of 5×1 excited S-layer elements of different orientations were considered as bar stimuli. Sets of excited S-layer elements belonging to half-planes with different oriented boundaries served as edge stimuli. Excitation of 3×3 S-layer elements was considered as a diffuse stimulus. Stimuli which were orthogonal to the strongest inhibition direction were considered to be optimally oriented. Figure 3 displays responses of E-layer neurons which receive projections from centers of each stimuli.

The analysis of neuron responses in our computer simulations revealed the following:

(1) Neuron responses to optimally oriented stimuli had sustained or biphase character. Neuron responses to otherwise oriented stimuli were transient and monophase.

(2) The later phases of neuron responses were much more sensitive to the stimulus orientation than the initial phases.

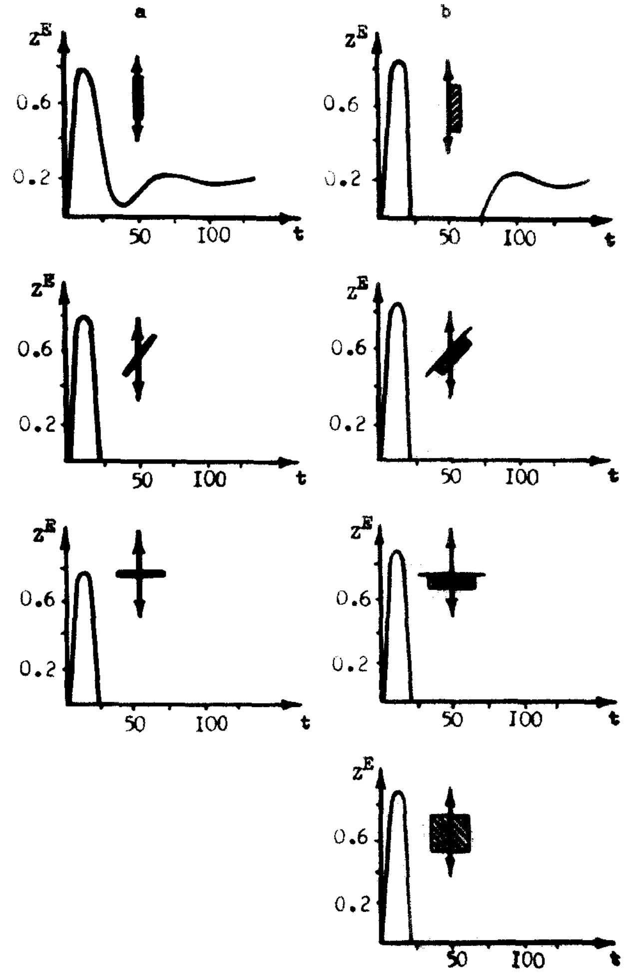

FIGURE 3. Responses of E-layer neurons to optimally (at the top), non-optimally (in the middle) oriented bars (a) and edges (b) and to diffuse stimulation (at the bottom). The curves correspond to the following values of parameters: $N = 16$; $k = 1$; $q^{EE} = 0.1$; $q^{IE} = 1$; $q^{SE} = 1$; $q_0^{EI} = 1.5$; $q^{EI} = 5$; $T_E = 10$; $T_I = 40$; $Z_m = 1$.

4. NEUROPHYSIOLOGICAL RESULTS

Neurophysiological experiments were carried out (Rybak, 1988; Rybak, Shevtsova, Podladchikova, Golovan, & Markarov, 1987) to study response dynamics and orientation sensitivity of neurons of the guinea-pig visual cortex (area 17). Light bars of different orientations were presented for 1 sec. Only on-responses of registered neurons were analyzed here. Figures 4 and 5 illustrate response histograms of some visual cortex neurons and diagrams of their tuning to stimulus orientation depicted for the overall response and for its separate phases.

The results of experiments supported (1) and (2). The analysis of the experimental findings showed that 73% of all orientation-selective neurons, or 85% of those which had later phases in their responses, displayed responses in which later phases had a more sharp tuning to stimulus orientation than initial ones.

Comparison of these results with the known data on orientation selectivity in the visual cortex is rather difficult for several reasons. In particular, the orientation tuning was often estimated over the entire response without its subdivision into phases. Besides, most of the authors used either moving stimuli or stimuli presented for a short time (less 100 ms). However, when moving oriented stimulus is presented, response dynamics depends also on directional properties of cortical and subcortical neurons. When short-time stimulus is presented, the later phase of on-response may be reduced and mixed with off-response. Nevertheless, Creutzfeldt and Ito (1968) revealed a presence of initial phases in responses to nonoptimal stimuli. Moreover, Supin (1974) assumed that many stimulus parameters had a much stronger effect upon the later temporal component of response than upon the initial one. Our findings also resemble data of Pubols and Leroy (1977) on orientation selectivity of somatosensory cortex neurons.

Results of our study indicate that there is the temporal discrimination of image features in the visual cortex. The initial phase of response of an iso-ori-

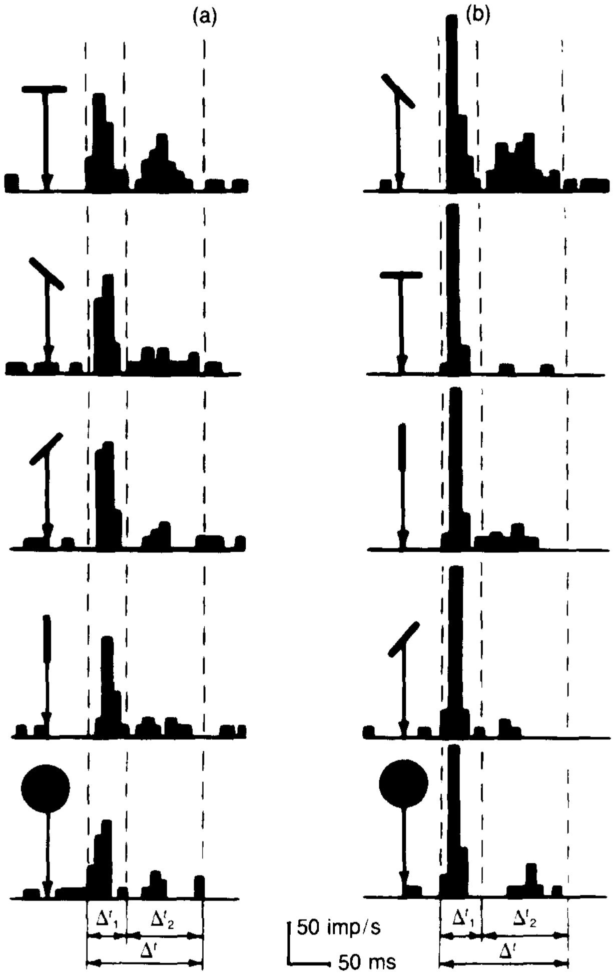

FIGURE 4. Histograms of responses of two neurons (a,b) in the guinea-pig visual cortex to optimally (at the top) and non-optimally (in the middle) oriented light bars and a diffuse stimulus (at the bottom). Onset of stimulation is indicated by the vertical arrow; Δt, Δt_1, Δt_2,—assumed durations of the overall response and its initial and later phases, respectively. Vertically plotted lines separate the phases of responses.

entation domain may encode appearance of a stimulus in the receptive field of the hypercolumn, whereas the later phase of the response may encode existence of contrast or contour image elements oriented in accordance with the domain orientation tuning.

5. SCREEN-TYPE NEURON-LIKE STRUCTURE AS A FUNCTIONAL UNIT OF THE MODEL OF THE NEURAL VISUAL PREPROCESSOR

A model of screen-type neuron-like structure (SNS) was developed on the basis of the model of the iso-orientation domain described above. It was assumed that the SNS had the same function in the preprocessor as the iso-orientation domain (orientation-selective column) had in the visual cortex. The SNS model consisted of 25 (5×5) neuron-like elements arranged in a flat layer (Figure 6). Each SNS transformed an 5×5 input signal matrix $S = \|S_{ij}\|$ into an output matrix $Z = \|Z_{ij}\|$ of the same size. The

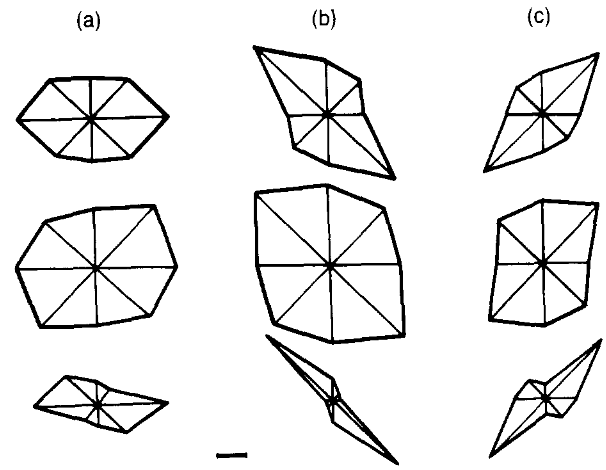

FIGURE 5. Diagrams of orientation tuning of three neurons (a,b,c) estimated on mean number of impulses over the entire response (at the top), over the initial phase (in the middle) and over the later phase (at the bottom). The scale mark corresponds to 10 impulses in the top row and five impulses in the others.

central 3×3 elements in matrix Z formed the operation area, while boundary elements served to eliminate possible edge distortion in data processing. The signals from the operation area passed into an output block which encoded information contained in the central 3×3 area of input matrix S. Each neuron-like element of the SNS was equivalent to a pair of neurons (E-layer neuron and corresponding I-layer neuron) (Figure 7). In order to reduce processing time, and taking into account (7), we put $T_E = 0$ and assumed E-layer neuron to be an inertialess threshold summarizing element. Input signals X_{ij}^S to each (i, j)-th element of the SNS passed through the F^S-block which performed spatial convolution with the input matrix S on the analogy of on-center/off-surround receptive field.

$$X_{ij}^S = S_{ij} - b_{ij}^S \sum_{k=\max(i-2;1)}^{\min(i+2;5)} \sum_{l=\max(j-2;1)}^{\min(j+2;5)} a_{k-i+3,l-j+3}^S S_{kl}, \quad (9)$$

where

$$b_{ij}^S = \left[\sum_{k=\max(i-2;1)}^{\min(i+2;5)} \sum_{l=\max(j-2;1)}^{\min(j+2;5)} a_{k-i+3,l-j+3}^S \right]^{-1}, \quad (10)$$

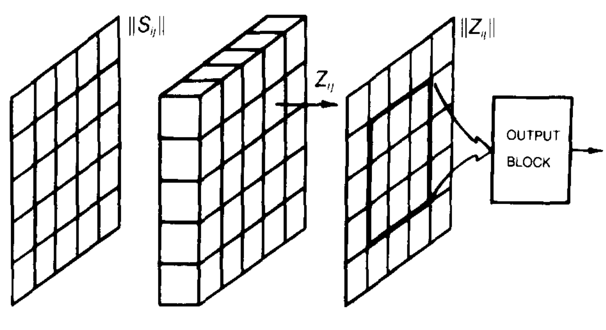

FIGURE 6. Screen-type neuron-like structure (SNS).

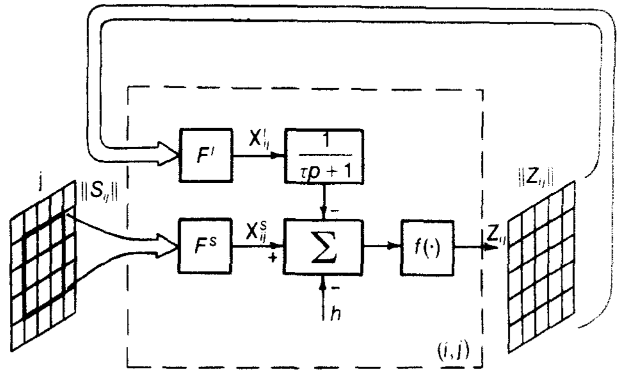

FIGURE 7. The (i,j)-th neuron-like element of the SNS.

where a^S_{pq} is element of matrix $A^S = \|a^S_{pq}\|$:

$$A^S = \|a^S_{pq}\| = \begin{Vmatrix} 0 & 0 & 0 & 0 & 0 \\ 0 & 1 & 1 & 1 & 0 \\ 0 & 1 & 0 & 1 & 0 \\ 0 & 1 & 1 & 1 & 0 \\ 0 & 0 & 0 & 0 & 0 \end{Vmatrix}. \tag{11}$$

According to (9)–(11), $X_{ij} > 0$ if S_{ij} exceeds the mean intensity level in the vicinity of the point (i,j).

Inertial backward inhibition affected the (i,j)-th element of the SNS through the block F^l which performed spatial convolution with the output matrix Z. Coefficients of the convolution matrix determined anisotropy of lateral inhibition.

$$X^l_{ij} = b^l \sum_{k=\max(i-2;1)}^{\min(i+2;5)} \sum_{l=\max(j-2;1)}^{\min(j+2;5)} a^l_{k-i+3,l-j+3}(\varphi) Z_{kl}, \tag{12}$$

where b^l is weight coefficient characterizing backward inhibition. It is similar to β in (6) and is chosen so that $b^l > 1$. $a^l_{pq}(\varphi)$ is element of coefficient matrix $A^l_\varphi = \|a^l_{pq}\|_\varphi$ which provides the orientation tuning of the SNS at an angle φ:

$$A^l_{\varphi=0^\circ} = \|a^l_{pq}\|_{\varphi=0^\circ} = \begin{Vmatrix} 1 & 0 & 0 & 0 & 1 \\ 1 & 1 & 0 & 1 & 1 \\ 1 & 1 & 0 & 1 & 1 \\ 1 & 1 & 0 & 1 & 1 \\ 1 & 0 & 0 & 0 & 1 \end{Vmatrix};$$

$$A^l_{\varphi=90^\circ} = (A^l_{\varphi=0^\circ})^T;$$

$$A^l_{\varphi\cong30^\circ} = \|a^l_{pq}\|_{\varphi\cong30^\circ} = \begin{Vmatrix} 1 & 1 & 1 & 0 & 0 \\ 1 & 1 & 0 & 0 & 1 \\ 1 & 1 & 0 & 1 & 1 \\ 1 & 0 & 0 & 1 & 1 \\ 0 & 0 & 1 & 1 & 1 \end{Vmatrix};$$

$$A^l_{\varphi\cong60^\circ} = (A^l_{\varphi\cong30^\circ})^T;$$

$$A^l_{\varphi\cong120^\circ} = \|a^l_{pq}\|_{\varphi\cong120^\circ} = \begin{Vmatrix} 0 & 1 & 1 & 1 & 1 \\ 0 & 0 & 1 & 1 & 1 \\ 1 & 0 & 0 & 0 & 1 \\ 1 & 1 & 1 & 0 & 0 \\ 1 & 1 & 1 & 1 & 0 \end{Vmatrix};$$

$$A^l_{\varphi\cong150^\circ} = (A^l_{\varphi\cong120^\circ})^T. \tag{13}$$

Let input signal matrix S be presented to the SNS input at the moment t_o. Then dynamics of SNS elements at $t > t_o$ is defined by partial solution of following system of differential equations:

$$\tau \frac{d}{dt} U_{ij} = -U_{ij} + X^S_{ij} - X^l_{ij} - h;$$
$$Z_{ij} = f[U_{ij}]; \qquad i,j = 1, \ldots, 5, \tag{14}$$

under initial conditions

$$U_{ij}(t_o) = X^S_{ij} - h; \qquad i,j = 1, \ldots, 5, \tag{15}$$

where τ is time constant of inertial block and h is threshold of summarizing element.

Each (i,j)-th element of the SNS displays either monophase (Figure 8a) or biphase (Figure 8b) responses. The intensities of initial and later phases have been estimated by values Z_{ij} at moments t_o and t_1, respectively. Here, t_o is the initial moment of stimulation. The moment t_1 is chosen experimentally to be the same for all elements of the SNS and for all parameters of stimuli presented ($t_1 \cong t_o + 5\tau$).

Let us consider the SNS tuned to vertical stimulus orientation (Figures 8c–f). Output of the SNS $Z = \|Z_{ij}\|$ at time moments t_o and t_1 depends on input

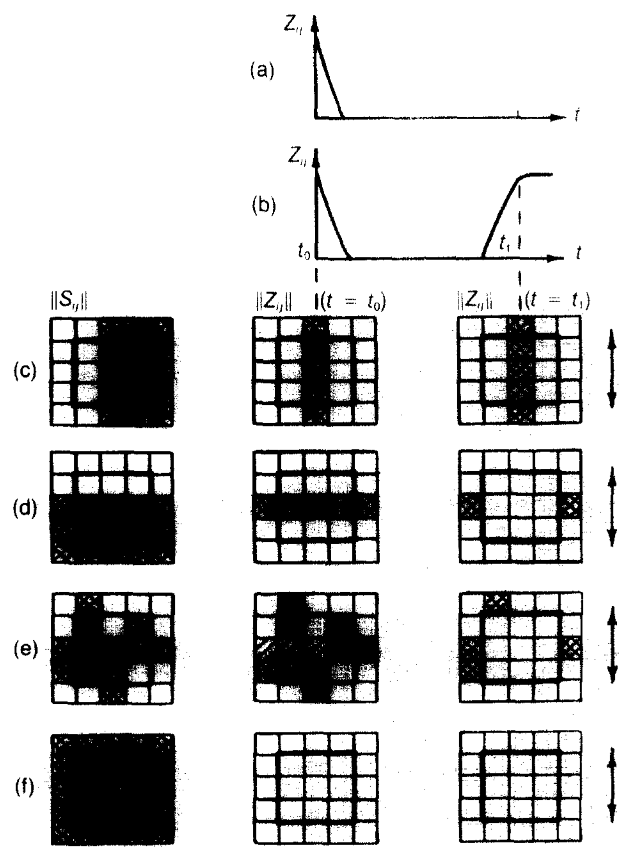

FIGURE 8. Dynamics of SNS responses: a,b—two types of dynamic responses of SNS elements; c–f—output SNS responses to different input stimuli; density of shading reflects intensities of S_{ij} and Z_{ij}.

matrix $S = \|S_{ij}\|$. At t_0, the operation area of output matrix Z contains some excited elements only if intensity differencies between S_{ij} are greater than the threshold h (Figures 8c–e). At t_1, the operation area of Z contains three excited elements only if there is an optimally oriented edge in S (Figure 8c). Otherwise, at t_1, the number of excited elements in Z is less (Figures 8d–f).

Thus, each SNS is at first a detector of suprathreshold intensity differencies and then it is a detector of the edge of certain orientation.

6. MULTIRESOLUTION CONTOUR FEATURE ENCODING AND PARALLEL-SEQUENTIAL ANALYSIS OF VISUAL INFORMATION

Trying to achieve likeness, an artist usually follows the way which may be called "coarse-to-fine." Throughout this process, he draws a number of auxiliary line segments of different lengths being the elements of more generalized contours of objects depicted. Spatial relationships between the elements of generalized contours play a very important role in making a true picture of the object. The estimation of spatial relations between the elements of coarser and finer contours are also important. Moreover, it should be noted that the artist achieves expressiveness and likeness by omitting some details of the picture and concentrating on its most informative parts.

It is tempting to assume that the artist intuitively employs the algorithms of visual perception, including sequential eye fixations. It is well known (Yarbus, 1965) that when a man is viewing an object, he performs certain eye movements and fixes his gaze on the most informative image fragments (Figure 9). During eye fixations these fragments are projected onto the fovea which has hyperrepresentation in the visual cortex (Talbot & Marshall, 1941; Yarbus, 1965). Due to such organization of the projections, these fragments may be processed at the highest resolution level. Besides, in the course of consecutive eye fixations, the same parts of the image are repeatedly projected onto the retina at different distances from its center and are processed in the cortex at various levels of resolution. Evidently, the set of iso-orientation domains in different parts of the visual cortex may encode orientations of contour elements of various degrees of generalization. Encoding spatial relationships between coarser elements, as well as between those and finer contour elements, leads to formation of a set of primary features for the invariant shape representation. A substantial reduction of information may be achieved due to omitting a higher resolution level processing of fragments which are less significant for object recognition.

Taking into account the above mentioned, it is reasonable to suggest that two phases of responses of a set of iso-orientation domains (hypercolumn), processing a fragment of an image in a parallel way, transmit different information to higher level of the visual system. The initial phases contain the information about the presence of brightness relief in the fragment and may be used by the oculomotor system in sequential procedure of image viewing. On the other hand, the later phases contain the information about a set of orientations of contour and edge elements in the fragment.

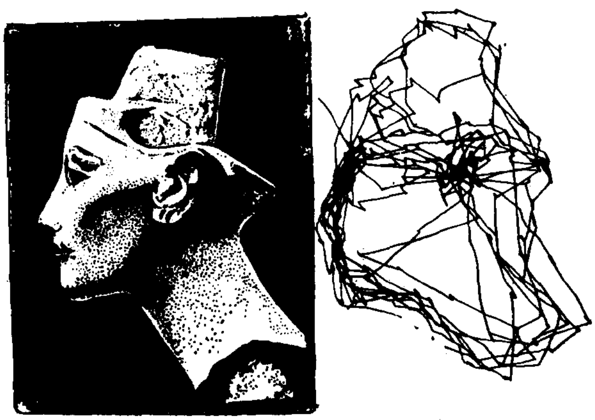

FIGURE 9. Trajectory of eye movements and gaze fixations during recognition of image by man (Yarbus, 1965).

7. NEURAL PREPROCESSOR IN THE SYSTEM OF IMAGE ANALYSIS

The proposed model of image processing is based on image features extraction at different levels of resolution. The method of multiresolution image processing in computer vision has several advantages (Burt, 1988; Levialdi, 1983; Rosenfeldt, 1984). For instance, this method allows the extraction of global features of images by local operators applied at lower resolution levels and to represent images by a set of

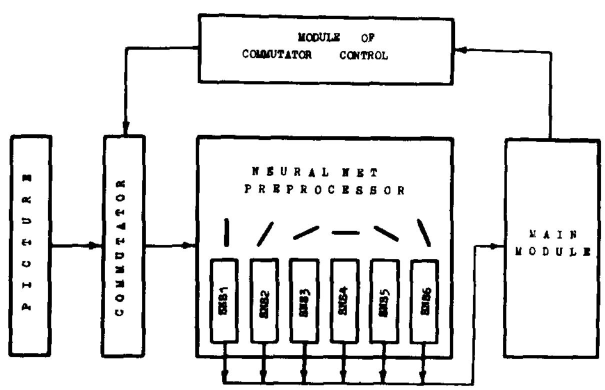

FIGURE 10. Block diagram of the system of image analysis.

FIGURE 11. Test image.

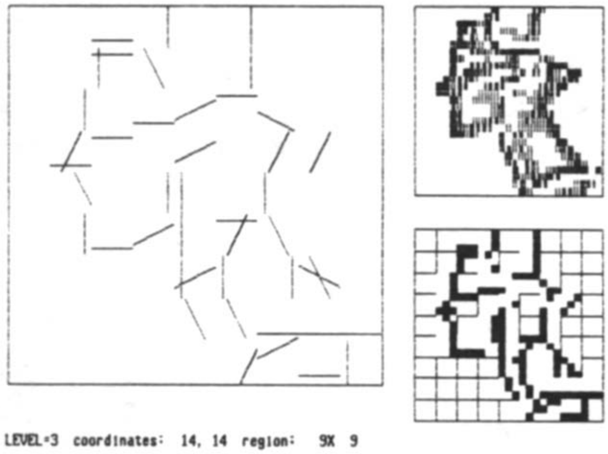

FIGURE 12. Visualized results of sequential processing of the test image at the third level of resolution (on the left). The results of sequential processing of fragments at initial moments t_0 are shown in the top right-hand corner. Summarized results of sequential processing of fragments by all SNSs at later moments t_1 are shown in the bottom right-hand corner.

boundary segments of different scales (Neveu, Dyer, & Chin, 1985; Schneier, 1984).

Figure 10 shows a block diagram of the proposed system of image analysis. The test image was presented in the maximal resolution raster of 243 × 243 pixels. The commutator module, directing the preprocessor to process the part of the image, played the role of the oculomotor system. The module of commutator control set the resolution level, size of the processed image part and its position in the raster. The raster of each resolution level contained $3^n \times 3^n$ pixels, where n was the resolution level number ($n = 1, \ldots, 5$). Stimulus intensity in each point of the raster of the lower resolution level was defined by averaging the intensity over nine (3 × 3) corresponding points of the higher resolution level raster. Hereby

$$S_{ij}(n) = \frac{1}{9} \sum_{k=3i-2}^{3i} \sum_{l=3j-2}^{3j} S_{kl}(n+1), \qquad n = 1, 2, 3, 4. \qquad (16)$$

At each step of sequential processing, a fragment of 5 × 5 elements was presented to the input of the neural network preprocessor. The preprocessor consisted of six SNSs tuned to different orientations in range from 0° to 180°. At the initial moment, the SNSs provided information about intensity differences in the fragment, and then they performed discrimination and encoding contour element orientations within the fragment. On the basis of information from the preprocessor, the data on the fragment position in the raster and on the resolution level, the

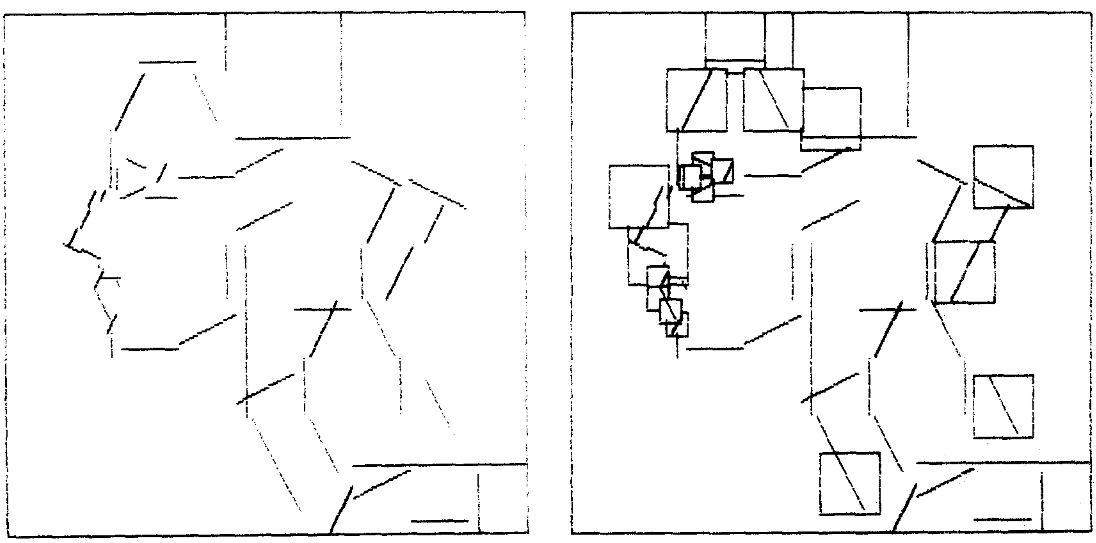

FIGURE 13. Visualized results of test image processing at the third resolution level and additional processing of some fragments at the third and fourth resolution levels. On the right, additionally processed fragments are framed.

main module may compute spatial relationships between contour elements extracted at the present step and elements detected at other steps. By the comparison of the processing results with the template information, the main module should determine the strategy of future steps of the sequential image analysis.

Figure 12 shows the results of sequential processing of the test image of Nefertiti's head (Figure 11) at the third level of resolution. Figure 13 represents the result of processing of the whole image at the third level with additional processing of some fragments at the third and fourth resolution levles. Visualized results of processing presented here seem to be quite sufficient for recognition of test image. Our future efforts will be focused on the following problems:

1. Segmentation of extracted image elements;
2. Development of strategy of sequential image processing;
3. Realization of higher level algorythms for the main module of the system.

REFERENCES

Amari, S. (1977). Dynamics of pattern formation in lateral-inhibition type neural fields. *Biological Cybernetics*, **27**, 77–87.

Amari, S. (1982). Competitive and cooperative aspects in dynamics of neural excitation and self-organization. *Lecture Notes in Biomathematics*, **45**, 1–28.

Baxter, W. T., & Dow, B. M. (1989). Horizontal organization of orientation-sensitive cells in primate visual cortex. *Biological Cybernetics*, **61**, 171–182.

Benevento, L. A., Creutzfeldt, O. D., & Kuhnt, U. (1972). Significance of intracortical inhibition in the visual cortex. *Nature*, **238**, 124–126.

Braitenberg, V., & Braitenberg, C. (1979). Geometry of orientation columns in the visual cortex. *Biological Cybernetics*, **33**, 179–186.

Burt, P. J. (1988). Smart sensing within a pyramidal vision machine. *Proceedings of the IEEE*, **76**, 970–981.

Creutzfeldt, O., & Ito, M. (1968). Functional synaptic organization of primary visual cortex neurones in the cat. *Experimental Brain Research*, **6**, 324–352.

Creutzfeldt, O., Kuhnt, U., & Benevento, L. A. (1974). An intracellular analysis of visual cortical neurones to moving stimuli: responses in a cooperative neuronal network. *Experimental Brain Research*, **21**, 251–274.

Eccles, J. C. (1969). *The inhibitory pathways of the central nervous system*. Liverpool, UK: Liverpool University Press.

Ferster, D., & Lindstrom, S. (1983). An intracellular analysis of geniculo-cortical connectivity in area 17 of the cat. *Journal of Physiology*, **342**, 181–215.

Finette, S., Harth, E., & Csermely, T. J. (1978). Anisotropic connectivity and cooperative phenomena as a basis for orientation sensitivity in the visual cortex. *Biological Cybernetics*, **30**, 231–240.

Garey, L. G., & Powell, T. P. S. (1971). An experimental study of the termination of the lateral geniculo-cortical pathway in the cat and monkey. *Proceedings of the Royal Society of London, Series B*, **119**, 41–63.

Grossberg, S., Mingolla, E., & Todorovic, D. (1989). A neural network architecture for preattentive vision. *IEEE Transaction on Biomedical Engineering*, **36**, 65–84.

Hayashi, Y. (1969). Recurrent collateral inhibition of visual cortical cells projecting to superior colliculus in cats. *Vision Research*, **9**, 1367–1380.

Hess, R., Negishi, K., & Creutzfeldt, O. (1975). The horizontal spread of intracortical inhibition in the visual cortex. *Experimental Brain Research*, **22**, 415–419.

Hubel, D. H., & Wiesel, T. N. (1962). Receptive fields, binocular integration and functional architecture in the cat's visual cortex. *Journal of Physiology*, **160**, 106–154.

Hubel, D. H., & Wiesel, T. N. (1974). Sequence, regularity and geometry of orientation columns in the monkey striate cortex. *Journal of Comparative Neurology*, **158**, 267–293.

Ito, M. (1970). Neuronal linkage in the cat visual cortex. *Journal of Physiological Society of Japan*, **32**, 550–551.

Julesz, B. (1975). Experiments in the visual perception of texture. *Scientific American*, **232**, 34–43.

Kohonen, T. (1988). An introduction to neural computing. *Neural Networks*, **1**, 3–16.

Kunt, M., Ikonomopoulos, A., & Kocher, M. (1985). Second-generation image coding techniques. *Proceedings of the IEEE*, **73**, 549–574.

Levialdi, S. (1983). Neighbourhood operators: an outlook. In Pictorial Data Analysis. *Proceedings of NATO Advanced Study Institute* (F4 pp. 1–14), West Berlin.

Linsker, R. (1986a). From basic network principles to neural architrecture: emergence of orientation-selective sells. *Proceedings of the National Academy of Sciences*, **83**, 8390–8394.

Linsker, R. (1986b). From basic network principles to neural architrecture: emergence of orientation columns. *Proceedings of the National Academy of Sciences*, **83**, 8779–8783.

Malsburg, Chr. von der (1973). Self-organization of orientation sensitive cells in the striate cortex. *Kybernetik*, **14**, 85–100.

Malsburg, Chr. von der & Cowan J. D. (1982). Outline of a theory for the ontogenesis of iso-orientation domains in the visual cortex. *Biological Cybernetics*, **45**, 49–56.

Minsky, M. (1975). A framework for representing knowledge. In P. H. Winston (Ed.) *The Psychology of Computer Vision* (pp. 211–277). New York: McGraw-Hill.

Neisser, V. (1967). *Cognitive psychology*. New York: Appleton.

Neveu, C. G., Dyer, C. R., & Chin, R. T. (1985). Object recognition using Hough pyramids. *In Proceedings of the Computer Society Conference on Computer Vision and Pattern Recognition* (pp. 328–333). San Francisco.

Paradiso, M. A. (1988). A theory for the use of visual orientation information which exploits the columnar structure of striate cortex. *Biological Cybernetics*, **58**, 35–49.

Pubols, L. M., & Leroy, R. F. (1977). Orientation detectors in the primary somatosensory neocortex of the raccoon. *Brain Research*, **129**, 61–74.

Rosenfeldt, A. (Ed.). (1984). *Multiresolution image processing and analysis*. New York: Springer-Verlag.

Rybak, I. A. (1988). *Study of response dynamics and orientation selectivity of visual cortex neurons by methods of mathematical modelling and neurophisiological experiment*. Doctoral thesis, Rostov-on-Don, USSR (in Russian).

Rybak, I. A., Shevtsova, N. A., Podladchikova, L. N., Golovan, A. V., & Markarov, V. G. (1987). Modelling and study of response dynamics and mechanisms of the preprocessing of sensory information in the screen-type neural structures. In All-Union Institute for Scientific and Technical Information. USSR, N 1657-B87 (in Russian).

Schwartz, F. L. (1980). A quantitative model of the functional architecture of human striate cortex with application to visual illusion and cortical texture analysis. *Biological Cybernetics*, **37**, 63–76.

Shiffrin, R. M., & Schneider, W. (1977). Controlled and automatic human information processing. 2. Perceptual learning, auto-

matic attending, and a general theory. *Psychological Review*, **84**, 127–190.
Shneier, M. (1984). Multiresolution feature encodings. In A. Rosenfeldt (Ed.) *Multiresolution Image Processing and Analysis* (pp. 190–199), New York: Springer-Verlag.
Sillito, A. M. (1975). The contribution of inhibitory mechanisms to the receptive field properties of neurones in striate cortex of the cat. *Journal of Physiology*, **250**, 305–329.
Sillito, A. M. (1984). Functional considerations of the operation of GABAergic inhibitory processes in the visual cortex. In *Cerebral Cortex* (Vol. 2, pp. 91–117), New York, London: Plenum Press.
Stefanis, C., & Jasper, H. (1964). Recurrent collateral inhibition in pyramidal tract neurons. *Journal of Neurophysiology*, **27**, 855–877.
Supin, A. J. (1970). Feedback excitation and inhibition in the visual cortex. *Neurophisiologia*, **2**, 418–422 (in Russian).
Supin, A. J. (1974). Possible functional significance of different components of cortical unit responses to patterned visual stimuli. *Sechenov Physiological Journal of the USSR*, **60**, 1634–1640 (in Russian).
Talbot, S. A., & Marshall, W. H. (1941). Physiological studies on neural mechanisms of visual localization and discrimination. *American Journal of Physiology*, **24**, 1255–1263.
Vidyasagar, T. R. (1987). A model of striate response properties based on geniculate anisotropies. *Biological Cybernetics*, **57**, 11–23.
Watanabe, S., Konishi, M., & Creutzfeldt, O. D. (1966). Postsynaptic potentials in the cat's visual cortex following electrical stimulation of afferent volleys. *Experimental Brain Research*, **1**, 272–283.
Wilson, H. R., & Cowan, J. D. (1972). Excitatory and inhibitory interactions in localized populations of model neurons. *Biophysical Journal*, **12**, 1–24.
Wilson, H. R., & Cowan, J. D. (1973). A mathematical theory of the functional dynamics of cortical and thalamic nervous tissue. Kybernetik, **13**, 55–80.
Yarbus, A. L. (1965). *The role of eye movements in vision process*. Moscow, USSR: Nauka (in Russian).

NOMENCLATURE

t: time variable.
t_0: initial moment of stimulation in the SNS model. Intensities of initial phases of SNS element responses have been estimated at the same moment.
t_1: moment of time. Intensities of SNS element later phases have been estimated at this moment.
Δt, Δt_1, Δt_2: assumed durations of the overall response of neuron and its initial and later phases respectively (in experimental research).
T_i: time constant of the i-th neuron.
T_E, T_I: time constants of neurons in E- and I-layers respectively.
τ: time constant of the inertial block of the SNS.
U_i: membrane potential of the i-th neuron.
U^E_{ij}, U^I_{ij}: membrane potentials of the (i,j)-th neurons in E- and I-layers respectively.
Z_i: output variable (frequency of impulses) of the i-th neuron.
Z^E_{ij}, Z^I_{ij}: output variables of the (i,j)-th neurons in E- and I-layers respectively.
Z^S_{ij}: test input influence on the (i,j)-th neuron.
Z_m: value of $Z^S_{ij}(t)$ at $t \geq 0$.
Z_{ij}: element of output SNS matrix $Z = \|Z_{ij}\|$.
Z: output SNS matrix.
S_i: uncontrollable input influence on the i-th neuron.
S_E, S_I: uncontrollable input influences on neurons in E- and I-layers respectively.
S_{ij}: element of input SNS matrix $S = \|S_{ij}\|$.
S: input SNS matrix.
h_i: threshold of the i-th neuron.
h_E, h_I: thresholds of neurons in E- and I-layers, respectively.
h: threshold of SNS element.
q_{ij}: synaptic weight of the j-th input to the i-th neuron.
q^S_i: synaptic weight of the external input to the i-th neuron.
q^{EE}, q^{IE}, q^{EI}_0, q^{EI}, q: weights of synaptic connections between different layer

neurons: the first index letter stands for layer position of the postsynaptic neuron, the second index letter stands for that of presynaptic neuron.

X^S_{ij}: input signal to the (i,j)-th SNS element.

X^I_{ij}: inertial backward inhibition to the (i,j)-th SNS element.

φ: optimal stimulus orientation.

$\Omega_{ij}(\varphi)$: area of E-layer elements forming the excitatory inputs to the (i,j)-th I-layer neuron. It determines anisotropy of lateral inhibition corresponding to orientation φ.

a^S_{pq}: element of matrix $A^S = \|a^S_{pq}\|$.

$a^I_{pq}(\varphi)$: element of matrix $A^I_\varphi = \|a^I_{pq}\|\varphi$.

A^S, $A^I_{\varphi=\varphi_i}$: matrices.

α, β_0, β, b^S_{ij}, b^I, k: parameters.

N: $N \times N$ is the number of elements in each layer of the iso-orientation domain model.

n: number of resolution level.

i, j, k, l, p, q: indices.

$\dfrac{d}{dt}$: sign of derivative.

$f[\ ]$: sign of nonlinear function.

Σ: sign of summation.

$\max[a, b]$: sign of maximum of two values.

$A = \|a_{ij}\| = \begin{Vmatrix} a_{11} & \cdots & a_{1n} \\ \cdot & \cdots & \cdot \\ a_{n1} & \cdots & a_{nn} \end{Vmatrix}$: sign of matrix.

$(A)^T$: sign of matrix transposition.